Comparison of different models for predicting drainage relative permeability using pore scale numerical simulation of supercritical carbon dioxide and brine flow.

IOP Conf. Series: Materials Science and Engineering **495** (2019) 012111 doi:10.1088/1757-899X/495/1/012111

Comparison of different models for predicting drainage relative permeability using pore scale numerical simulation of supercritical carbon dioxide and brine flow.

S S Garimella[1,3], **S Ahmed**[2], **M M Hossain**[1]

[1] Curtin University, Kent St, Bentley WA 6102, Australia
[2] CSIRO, Kensington Street, Kent Street WA 6102, Australia
[3] saisravya.garimella@postgrad.curtin.edu.au

Abstract. In today's technologically growing and cost optimisation era, Digital Rock Physics (DRP) is becoming a potential alternative tool to the high cost and time-consuming method of Special Core Analyses (SCAL), for the estimation of reservoir fluid properties. The key objective of this study is to compare different models for predicting drainage relative permeability using pore scale numerical simulation of supercritical carbon dioxide and brine flow, the former being the non-wetting phase and the latter being the wetting phase. The simulations are done on an established computational fluid dynamics (CFD) simulator: ANSYS-CFX. From the simulations, we obtain the saturation values. Using these values and four common models found in the literature, we collaborate the J-function prediction model and capillary pressure values to calculate the relative permeability for the wetting and non-wetting phases. In this study, it is concluded that the Brooks-Corey-Burdine model produces the best relative permeability curves. It is demonstrated that the pore size distribution index ($\boldsymbol{\lambda}$) has a positive correlation with the wetting-phase relative permeability and an inverse relation with the non-wetting phase relative permeability. Noteworthy to mention that during the study, it was found that when the J-function is substituted into the relative permeability equations, the predicted relative permeabilities of wetting and non-wetting phase outcomes appears to be more representative, yet simple to compute. The robust methodology described in this paper to evaluate the simulation results with various established models is generic and could be useful in current day oil field practices to serve as a cost-effective alternative to SCAL experiments and form key inputs for typical oil field development planning.

1. Introduction

Digital Rock Physics (DRP) enhances our knowledge on interactions between pore-scale of the pore walls, water and oil. DRP is used to calculate properties in various fields: geology, reservoir and geophysical engineering. It can be used for solving problems that could be very expensive to conduct in the laboratories. The simulations carried out make it easier for the understanding of recovery mechanisms when the pore scale fluid distributions are analysed. DRP is being used by more and more companies that provide the imaging software and hardware, delivering computational services.

1.1. Drainage and Imbibition Process

In a porous media, the process of fluid flow where the non-wetting fluid displaces the wetting fluid is known as the drainage process. It could also be defined as the process where there is an increase in the saturation of the non-wetting phase and decrease in the saturation of the wetting phase [1]. This process is the main focus of this paper, where brine is the wetting phase and supercritical CO_2 (Sc CO_2) is the non-wetting phase. In a porous media, the process of fluid flow where the wetting fluid displaces the non-wetting fluid is known as the imbibition process. It can also be defined as the process where there is an increase in the saturation of the wetting phase and decrease in the saturation of the non-wetting phase [2]. The imbibition process is out of the scope of this paper.

1.2. Supercritical Carbon Dioxide

A lot of properties influence the injectivity of CO_2 – properties of the rock, host formation fluids, temperature and pressure [3]. Carbon dioxide, under reservoir conditions, is a supercritical fluid with critical pressure of 9 MPa and temperature of 31 ^{o}C. The solubility and density change significantly above and below the critical point [4]. Supercritical CO_2 tends to become denser when pressure increases to an extent where the density can cross that of water at standard temperature and pressure conditions [5]. Slight variations in temperature and pressure around the critical point leads to a meaningful change in the capillary pressure [6].

1.3. Relative Permeability Calculations

Relative permeability can be calculated in the laboratories using two principal methods: steady state and unsteady state [4]. Deep explanation of these methods is beyond the scope of this paper and hence will not be discussed extensively. Relative permeability is an extremely important parameter in the oil and gas industry, and for petroleum engineers. Over the years, several models have been proposed that deduce relative permeability, since conducting direct experiments have served to be difficult [7]. In 1993, Demond and Roberts compared different experimental measurements from four different methods: Purcell Model, Burdine Model, Corey Model and Brooks-Corey Model [8].

Relative permeability can also be calculated from numerical approaches like direct simulations and pore network modelling [9]. Deeper understanding and more information can be found in this reference [9].

2. Methodology

2.1. Rock Sample

For this study, a digital rock was analysed, a sand pack model with a measured permeability and porosity of 42 D and 33 % respectively. A detailed discussion of calculating porosity, absolute permeability and single-phase flow modelling can be found in Ahmed et al., 2012 [10]. This discussion emphasises on two phase numerical modelling using CFD.

2.2. Flow Analysis and Domain Conditions

The model was run under the transient condition with the initial time being 0 [s] and end time being 80 [s]. This condition was chosen as the simulations are time dependent. The time step was set to 0.01 [s] with 3 iterations, keeping a file after every 0.25 [s]. The CFX Command Language (CCL) has been attached in the Appendix A as reference for further information.

The model was selected to be a fluid domain and the morphology set to continuous fluid, with reference pressure of 1 MPa. All the other domain conditions are provided in Table 1. There is no gravity applied in the X and Z direction, only for the Y direction with a gravitational acceleration value of - 9.81 m/s^2. The domain motion remains stationary in regard to the reference frame.

Table 1. Domain conditions

Parameter	Value	Parameter	Value
Density (Brine)	990 kg/m^3	Surface tension co-efficient	0.0262 N/m
Density ($ScCO_2$)	490 kg/m^3	Drag Co-efficient	0.44

2.3. Boundary, Inlet and Outlet Conditions

Inlet, outlet and wall boundary conditions were specified. The contact angle is considered with a value of 15 degrees. The inlet flow regime is set to subsonic and a mass and momentum is considered to be fluid dependent. For the drainage process, the mass flow rate is chosen at the inlet. Brine has an initial mass flow rate of 0 kg/s with a volume fraction of 0. The mass flow rate of $ScCO_2$ is set to 1.0208E-06 kg/s with volume fraction as 1. It is essential for the volume fractions to add up to 1 [11]. The outlet boundary type is set to be an opening. The flow regime is subsonic, but the mass and momentum are an entrainment with a relative pressure of 9 MPa. At the outlet, the value of volume fraction for brine was set to 1 and that for the $ScCO_2$ was 0, since this is a drainage process [11].

2.4. Mathematical Model

In order to calculate the relative permeability for the wetting and non-wetting phases, the pore radius is calculated first, using equation (1). The radius (r) is calculated by choosing 10 diameters (D) from each face of the model and then averaged since the pore of the sand pack are not uniform. The model images for the diameter calculations are shown in Figure 1 – Figure 6.

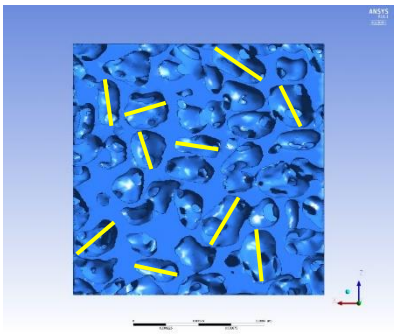

Figure 1: Face 1

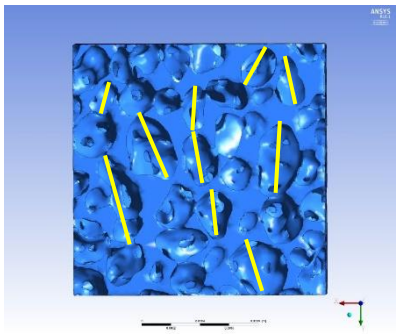

Figure 2: Face 2

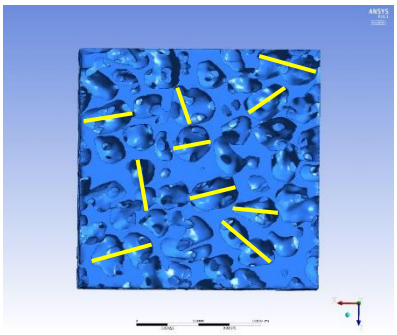

Figure 3: Face 3

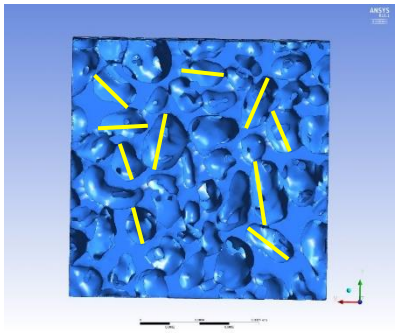

Figure 4: Face 4

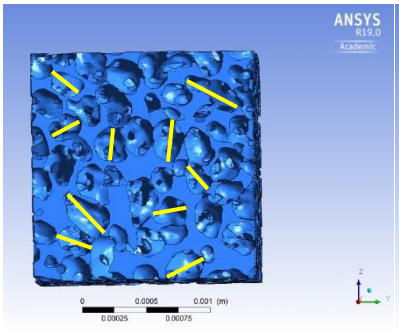

Figure 5: Face 5

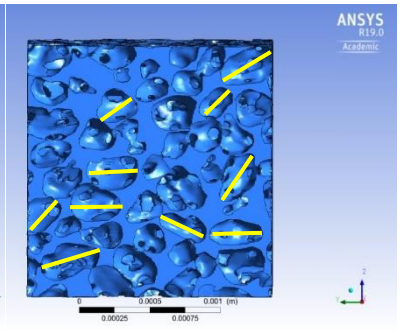

Figure 6: Face 6

Hence the diameter is calculated using below formula,

$$r = \frac{D}{2} \quad (1)$$

Capillary pressure (P_c) is then calculated using equation (2) given below.

$$P_c = \frac{2\sigma * \cos\theta}{\mathrm{r}} \tag{2}$$

Where, σ is the interfacial tension and θ is the contact angle.

Xu, et al. 2016 [12] developed a prediction model to calculate the relative permeability using the J-Function model. The J-Function model is a function of saturation, given by the equation (3) below:

$$J\,(S_e) = \; p_d \frac{\sqrt{\frac{k}{\Phi}}}{\sigma \cos\theta}\; {S_e}^{-1/\lambda} \tag{3}$$

Where, p_d is threshold pressure and S_e is normalized or effective saturation.

To calculate the relative permeability, four common models found in the literature were considered. Below are the equations for each model [7].

2.4.1 Purcell Model

Wetting phase relative permeability (k_{rw}):

$$k_{rw} \; = \; \frac{\int_0^{S_w} dS_w/(P_c)^2}{\int_0^1 dS_w/(P_c)^2} \tag{4}$$

Where, k_{rw} is the wetting phase relative permeability, S_w is the wetting phase saturation and P_c is the capillary pressure, as a function of S_w.

Non- wetting phase relative permeability (k_{rnw}):

$$k_{rnw} = \; \frac{\int_{S_w}^1 dS_w/(P_c)^2}{\int_0^1 dS_w/(P_c)^2} \tag{5}$$

In a study done by Horne 2006 [7], it was found that the numerical values for non-wetting phase relative permeability calculations are far from those of the experimental values [7]. It is also said that the Purcell model is far from the true rock pore structure since it is based on the principle of capillary bundle model [12].

2.4.2 Burdine Model

The tortuosity factor was derived from the Purcell Model, which is a function of the wetting phase saturation [13]. S_m is the minimum wetting phase saturation.

The tortuosity factor for the wetting phase is given by,

$$\lambda_{rw} \; = \; \frac{S_w - S_m}{1 - S_m} \tag{6}$$

Hence, the wetting phase relative permeability is given by,

$$k_{rw} \; = \; (\lambda_{rw})^2 \; \frac{\int_0^{S_w} dS_w/(P_c)^2}{\int_0^1 dS_w/(P_c)^2} \tag{7}$$

Following the same method, the tortuosity and relative permeability of the non-wetting phase can be calculated [7].

$$\lambda_{rnw} \; = \; \frac{1 - S_w - S_m}{1 - S_m - S_e} \tag{8}$$

S_e here represents the equilibrium saturation of the non-wetting phase. [7]

$$k_{rnw} = (\lambda_{rnw})^2 \frac{\int_{S_w}^{1} dS_w/(P_c)^2}{\int_{0}^{1} dS_w/(P_c)^2} \quad (9)$$

2.4.3 Corey Model

According to Burdine model, an analytical expression to calculate the relative permeability for the wetting phase and non-wetting phase could be obtained if the capillary pressure follows a simple mathematical function. In 1954, Corey [14] found that capillary pressure curves could be approximately expressed by the below function:

$$\frac{1}{P_c^2} = CS_e \quad (10)$$

The wetting phase relative permeability is given by:

$$k_{rw} = S_e^4 \quad (11)$$

The non-wetting phase relative permeability is given by:

$$k_{rnw} = (1 - S_e)^2 \, [1 - (S_e)^2] \quad (12)$$

2.4.4 Brooks-Corey-Burdine Model

The Brooks-Corey model is modified using the Burdine model, which is based upon the J-function prediction model, capillary pressure and saturation of wetting phase to obtain relative permeability [15]. Due to the limitation of Corey's capillary pressure equation, Brooks and Corey modified the Corey's model to produce a more generalized equation for capillary pressure. The capillary pressure curve is represented as a power law function of brine saturation. The equation for the new capillary pressure is given as:

$$P_c = p_e \, (S_e)^{-1/\lambda} \quad (13)$$

For the wetting phase relative permeability:

$$k_{rw} = S_e^{\frac{2+3\lambda}{\lambda}} \quad (14)$$

For the non-wetting phase relative permeability:

$$k_{rnw} = (1 - S_e)^2 \, [1 - (S_e)^{\frac{2+\lambda}{\lambda}}] \quad (15)$$

3. Results and Discussion

The model attained steady state at around 52 [s], after which the difference in the saturation of the wetting phase was negligible. The residual wetting phase saturation was 0.18. A $ScCO_2$ mass flow rate value of 1.0208 X 10^{-6} kg/s was not sufficient to drain all the brine out of the model, especially towards the outlet. This could also be because $ScCO_2$ is less dense in comparison to brine and needs a higher mass flow rate. Another reason could have been the boundary effect at the outlet. In the series of figures presented in the next page (Figure 7 – Figure 24), we noticed that, when the $ScCO_2$ is injected, it tends to move upwards first and then fills up at the bottom of the model. The reason for this is the force of gravity present only in the Y direction. The blue represents the volume fraction of brine and red represents the volume fraction of $ScCO_2$ filled in the model.

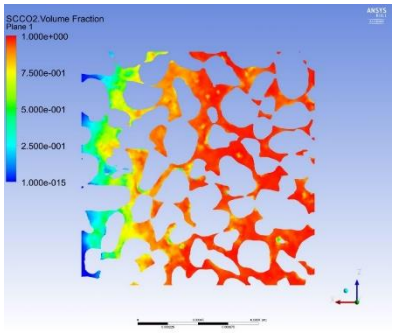

Figure 7: Plane view at 52 [s].

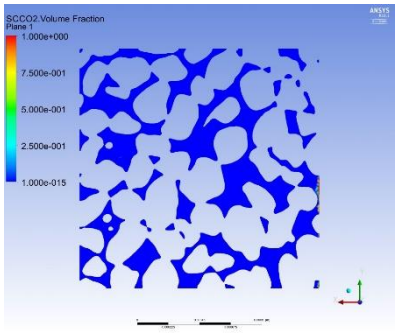

Figure 8: Plane view at 0 [s].

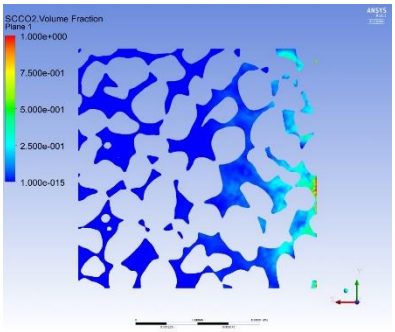

Figure 9: Plane view at 5 [s].

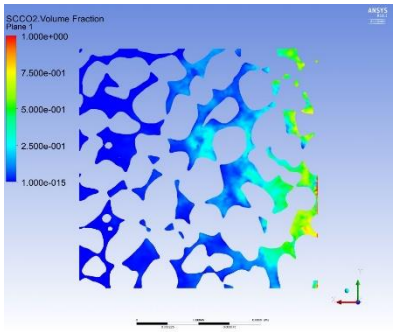

Figure 10: Plane view at 10 [s].

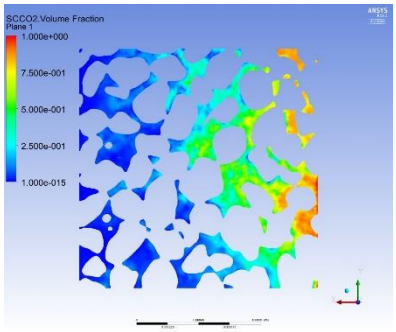

Figure 11: Plane view at 15 [s]

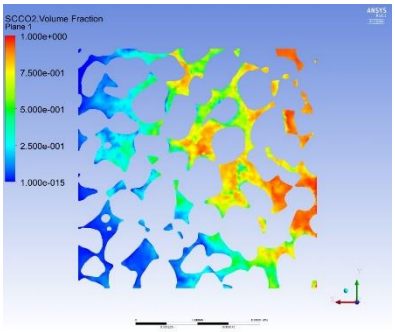

Figure 12: Plane view at 20 [s].

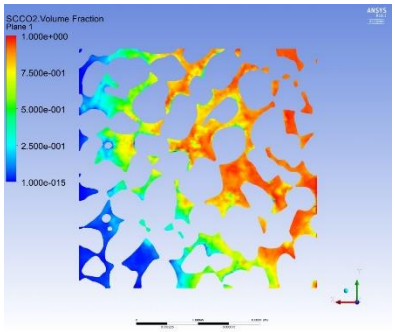

Figure 13: Plane view at 25 [s].

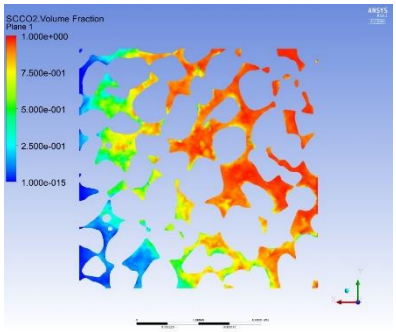

Figure 14: Plane view at 30 [s].

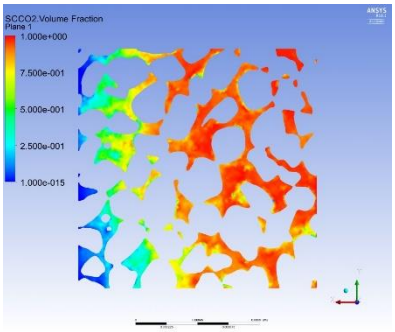

Figure 15: Plane view at 35 [s].

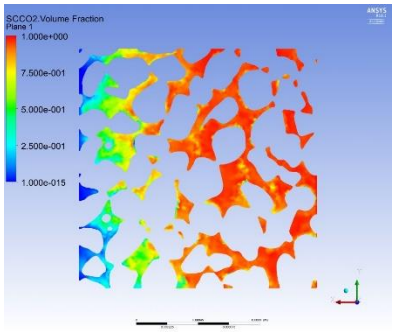

Figure 16: Plane view at 40 [s].

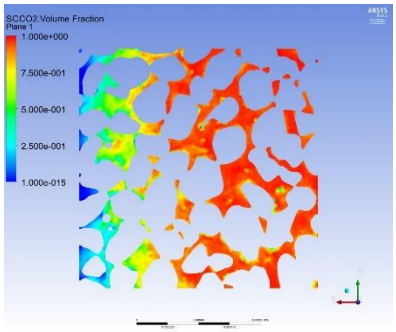

Figure 17: Plane view at 45 [s].

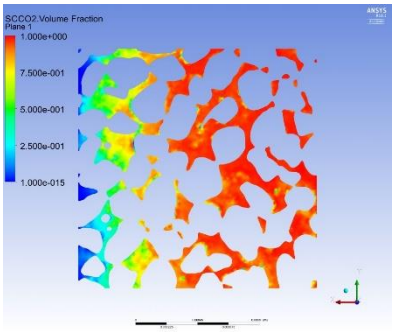

Figure 18: Plane view at 50 [s].

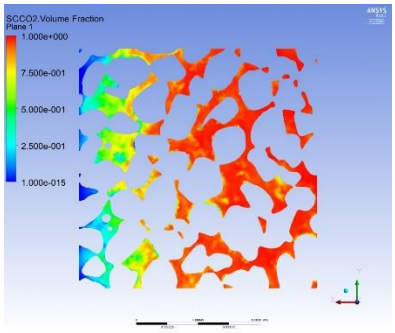

Figure 19: Plane view at 55 [s].

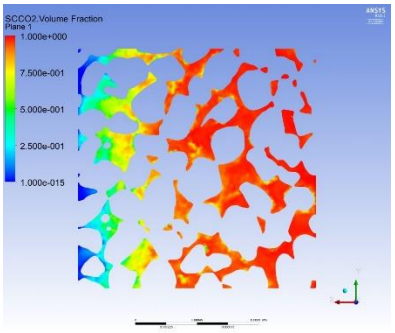

Figure 20: Plane view at 60 [s].

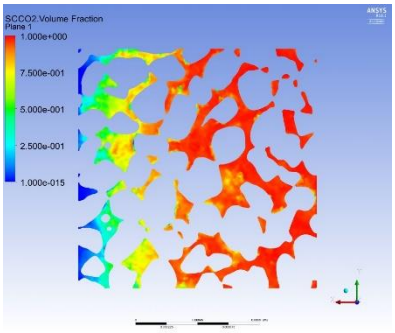

Figure 21: Plane view at 65 [s].

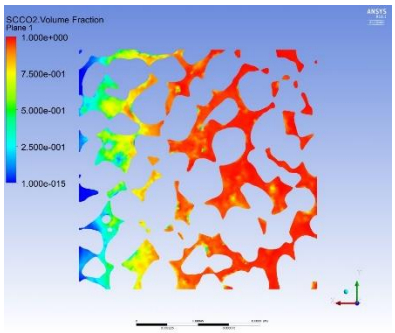

Figure 22: Plane view at 70 [s].

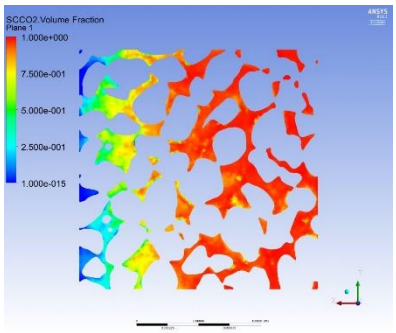

Figure 23: Plane view at 75 [s].

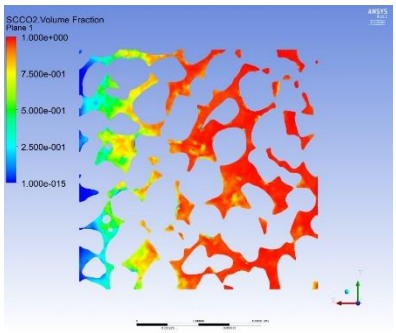

Figure 24: Plane view at 80 [s].

Substituting the values of all the parameters from Table 2, the J-Function curve was obtained as presented in Figure 25.

Table 2: Parameters for J-Function calculation

Parameter	Value	Parameter	Value
p_d	2.8 X 10^{-4} MPa	σ	0.0262 N/m
k	42 D	θ	15^o
ø	0.33	λ	0.5

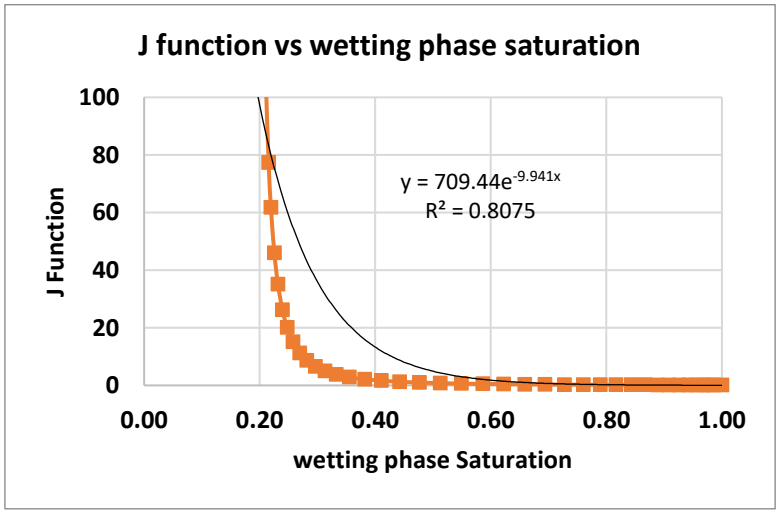

Figure 25: J-Function VS wetting phase plot

As for the relative permeability of the wetting and non-wetting phases are concerned, the plots are shown in Figures 26-29 for each of the four models described earlier.

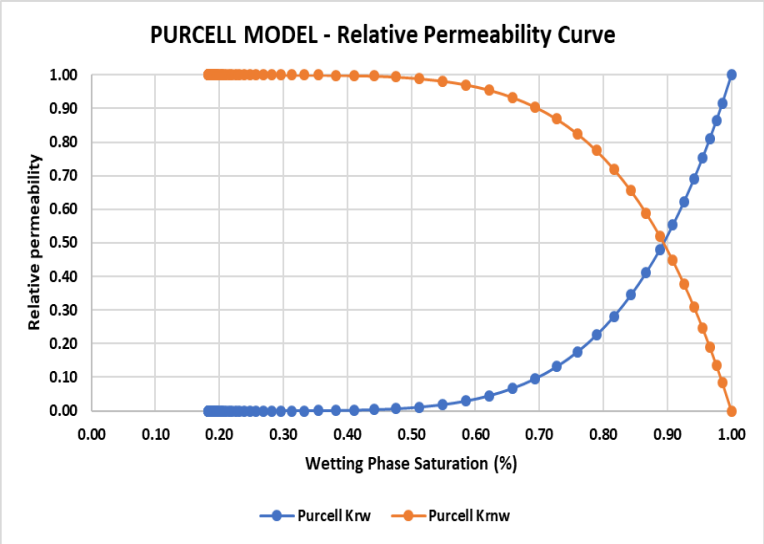

Figure 26: Purcell Model - Relative Permeability Curves

The non-wetting phase relative permeability curve does not follow the theoretical trend, for the Purcell model (Figure 26). Purcell's equation for the non-wetting phase relative permeability is reported to be not appropriate for experiment-based data as it is based on the capillary bundle model. [16]. The values are far off from each other when the experimental and numerical values were compared [7].

Introducing the tortuosity factor into the Purcell model gives us better results for the Burdine model. Assuming that the equilibrium saturation of the non-wetting phase is 0, the relative permeability calculations were conducted to obtain the relative permeability curves. A base case for value of $\boldsymbol{\lambda}$ = 0.5 is taken into account during calculations as this value was found to be the best fit in literature as well. Figure 27 depicts this.

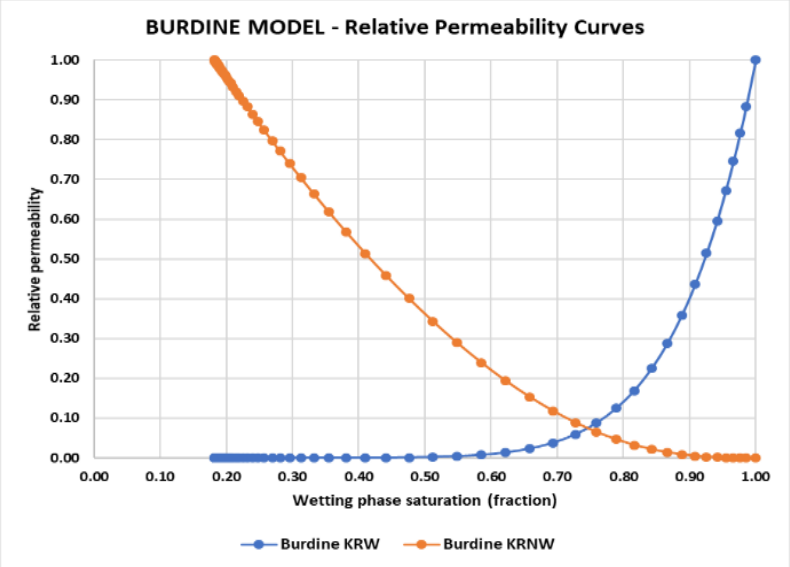

Figure 27: Burdine Model - Relative Permeability Curves

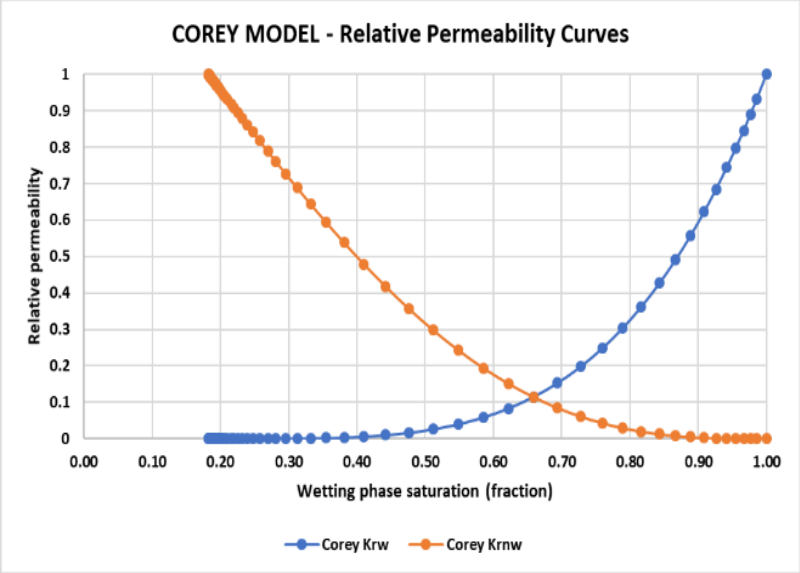

Figure 28: Corey Model - Relative Permeability Curves

The Corey model (Figure 28) is appeared to be independent of the pore size distribution index, which makes it an appropriate model for the calculations. However, due to the limitation of the capillary pressure curve being strictly represented by the curve, it is not preferred for obtaining the relative permeability curves. This model is independent of the pore size distribution index.

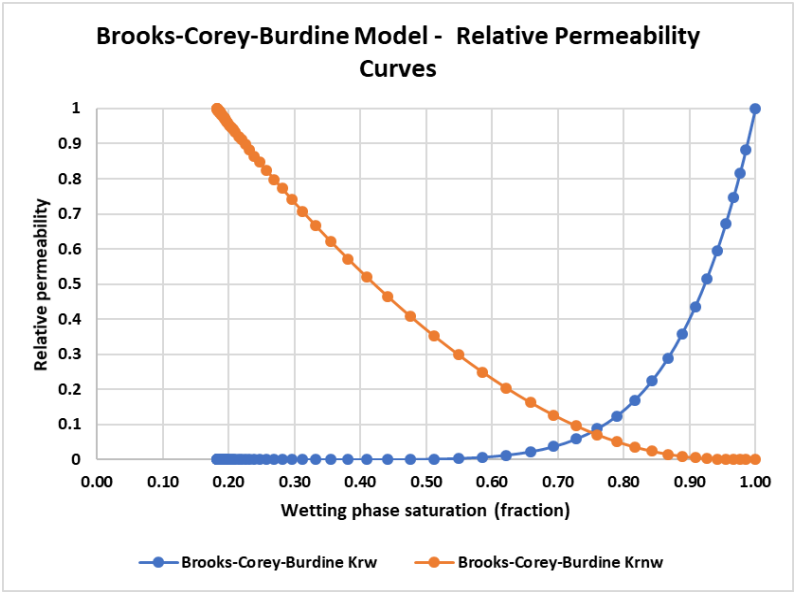

Figure 29: Brooks-Corey-Burdine Model - Relative Permeability Curves

Brooks-Corey Model is the most widely used in the industry. Substituting the J-function and calculating the relative permeability has proved to be simple to compute and is more representative. Combining the Burdine and Brooks-Corey model make it easier when substituting the J-function into the Burdine model. The relative permeability curves predicted using Brook-Corey-Burdine Model is presented in Figure 29.

A comparison was conducted by varying the value of the pore size distribution index for the Brooks-Corey-Burdine model. Two different values were taken into account, $\boldsymbol{\lambda}$ = 0.25 and $\boldsymbol{\lambda}$ = 0.75 apart from the initial assumption of $\boldsymbol{\lambda}$ = 0.5 In the Figure 30, we can see that the wetting phase relative permeability decreases when the value of $\boldsymbol{\lambda}$ decreases. The non-wetting phase relative permeability increases with decreasing value of $\boldsymbol{\lambda}$. We can clearly see that the wetting phase relative permeabilities differ in values whereas the non-wetting phase relative permeabilities are very close to each other.

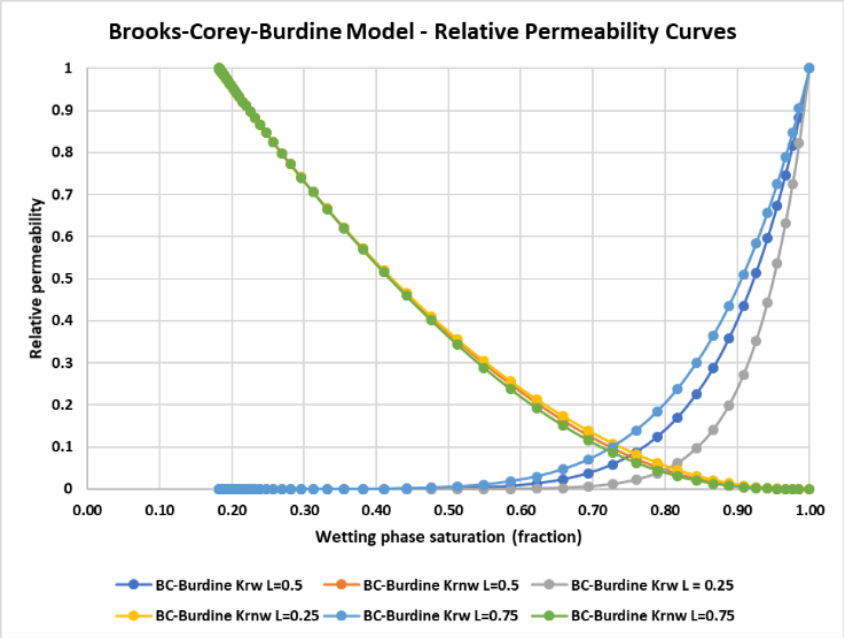

Figure 30: Brooks-Corey-Burdine Model - Relative Permeability Curves – Varying $\boldsymbol{\lambda}$

Figure 31 and Figure 32 show the initial (0 seconds) and final stage (80 seconds) of the drainage process, for the model. The flow is from right to left.

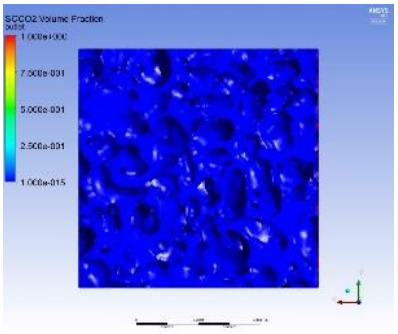

Figure 31: Initial Stage [10]

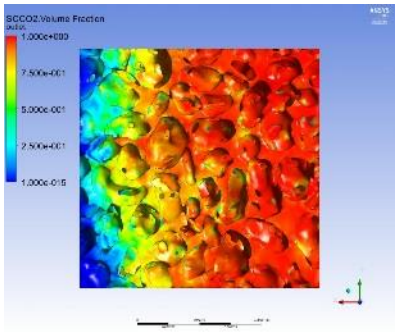

Figure 32: Final Stage [10].

4. Conclusions

In this paper, the ANSYS CFX simulator has been utilized in order to run the model for a two-phase flow of supercritical carbon dioxide ($ScCO_2$) and brine flow. The rock sample was segmented in CSIRO, Perth, using AVIZO. A successful drainage simulation was completed and the brine and $ScCO_2$ saturations were obtained from the model. A sand pack sample with measured permeability of 42 D and 33 % porosity was considered for this study. Best results were obtained by the Brooks-Corey-Burdine Model. CFD approach could be one of the best methods to generate related data as the values are promising and future research should be carried out to extend the applicability of this method on a larger scale. Digital rock physics and numerical simulation will be the future of the industry as they are cheaper and less time consuming when compared to laboratory experiments. It also provides the flexibility to conduct experiments with varying boundary conditions and explore their impacts on the relative permeability outcomes.

ACKNOWLEDGEMENTS

I would like to express my deepest gratification to my supervisors from CSIRO, Curtin University's Petroleum and Chemical Department. I would also like to thank the CITS department, Curtin University and CSIRO for providing me with all resources and facilities.

REFERENCES

[1] Dake, L., 1998. CHAPTER 4 - Darcy's Law and Applications. In: T. Y. a. G. CHILINGARIAN, ed. *FUndamentals of Reservoir Engineering.* The Hague: ELSEVIER

[2] Crain, 2017. *Crain's Petrophysical Handbook.* [Online] Available at: https://www.spec2000.net/09-wettability.htm [Accessed 15 May 2018].

[3] Dullien, F., 1992. *Porous Media: Fluid Transport and Pore Structure,* New York: Academic Press Inc.

[4] Muller, N., 2010. *Supercritical CO_2-Brine relative permeability experiments in reservoir rocks - literature review and recommendations,* Melbourne, Australia: Springer Science + Business Media.

[5] Pruess, N. S. a. K., 2004. *CO_2-H2O mixtures in the geological sequestration of CO_2. I. Assessment and calculation of mutual solubilities from 12 to 100°C and up to 600 bar. ,* Berkeley, California, USA : Lawrence Berkeley National Laboratory.

[6] Dake, L., 1978. *Fundamentals of Reservoir Engineering.*. Amsterdam,: New York: Elsevier Scientific Pub Co..
SCIENCE, pp. 100-126.

[7] Horne, K. L. a. R. N., 2006. Comparison of methods to calculate relative permeability from capillary pressure in consolidated water-wet porous media. *WATER RESOURCES RESEARCH,* VOL. 42,(W06405, doi:10.1029/2005WR004482,).

[8] Roberts, A. H. D. a. P. V., 1993. Estimation of 2-phase relative permeability relationships for organic liquid contaminants. *Water Resour,* Issue 29 (4), pp. 1081-1090.

[9] Arrufat, T. I. B. S. Z. U. P. M. C. B. L. a. N. K., 2014. *"Developments on relative permeability computation in 3D rock images,* Abu Dhabi: Abu Dhabi International Petroleum Exhibition and Conference..

[10] Ahmed , S., Iglauer, S , 2012. *Brine permeability predictions for sand packs and sandstones using Navier-Stokes equations and three-dimensional micro-tomography images of pore spaces,* 9th International conference on CFD in the Minerals and Process Industries, Melbourne, Australia.

[11] ANSYS, 2018. *About ANSYS.* [Online] Available at: https://www.ansys.com/about-ansys [Accessed 15 May 2018].

[12] Xu, W. S. P. Y. L. L. S. a. N. L., 2016. *A prediction model of capillary pressure J - Function,* Arizona, United States: PLOS One..

[13] Horne., K. L. a. R., 2002. *Experimental Verification of methods to calculate relative permeability using capillary pressure data.*. Anchorage, Alaska, Presentation SPE 76757, SPE Western Regional/AAPG Pacific section joint meeting..

[14] Corey, A. T., 1954. The Interrelation between gas and il relative permeabilities.. *PRODUCERS MONTHLY*.

[15] Honarpour, M. L. K. a. H. H. .., 1986. *Relative permeability of petroleum reservoirs.* Boca Raton: CRC Press..

[16] Li, Kewen, and Roland Horne. 2006. "Comparison of methods to calculate relative permeability from capillary pressure in consolidated water-wet porous media." *WATER RESOURCES RESEARCH* VOL. 42, W06405, doi:10.1029/2005WR004482.

Appendix A. CFX Command Language codes.

1. ANALYSIS TYPE

```
FLOW: Flow Analysis 1
&replace ANALYSIS TYPE:
Option = Transient
EXTERNAL SOLVER COUPLING:
Option = None
END
INITIAL TIME:
Option = Automatic with Value
Time = 60 [s]
END
TIME DURATION:
Option = Total Time
Total Time = 80 [s]
END
TIME STEPS:
Option = Timesteps
Timesteps = 0.01 [s]
END
END
END
```

2. DOMAIN

```
FLOW: Flow Analysis 1
&replace DOMAIN: F42voxel578
Coord Frame = Coord 0
Domain Type = Fluid
Location = Assembly
BOUNDARY: F42voxel578 Default
Boundary Type = WALL
Create Other Side = Off
Interface Boundary = Off
Location = F42 300VOXEL 578MICRON PORELESSMESH2 A
BOUNDARY CONDITIONS:
MASS AND MOMENTUM:
Option = No Slip Wall
```

END
WALL CONTACT MODEL:
Option = Use Volume Fraction
END
END
FLUID PAIR: Brine | SCCO2
BOUNDARY CONDITIONS:
WALL ADHESION:
Option = Adhesive
Wall Contact Angle = 15 [degree]
END
END
END
END
BOUNDARY: inlet
Boundary Type = INLET
Interface Boundary = Off
Location = ENTRANCE A
BOUNDARY CONDITIONS:
FLOW REGIME:
Option = Subsonic
END
MASS AND MOMENTUM:
Option = Fluid Velocity
END
END
FLUID: Brine
BOUNDARY CONDITIONS:
FLOW DIRECTION:
Option = Normal to Boundary Condition
END
VELOCITY:
Mass Flow Rate = 0 [kg s^-1]
Option = Mass Flow Rate
END
VOLUME FRACTION:
Option = Value
Volume Fraction = 0
END
END
END
FLUID: SCCO2
BOUNDARY CONDITIONS:
FLOW DIRECTION:
Option = Normal to Boundary Condition
END
VELOCITY:
Mass Flow Rate = 1.0208E-6 [kg s^-1]
Option = Mass Flow Rate
END
VOLUME FRACTION:
Option = Value
Volume Fraction = 1

END
END
END
END
BOUNDARY: outlet
Boundary Type = OPENING
Interface Boundary = Off
Location = EXIT A
BOUNDARY CONDITIONS:
FLOW REGIME:
Option = Subsonic
END
MASS AND MOMENTUM:
Option = Entrainment
Relative Pressure = 9 [MPa]
END
END
FLUID: Brine
BOUNDARY CONDITIONS:
VOLUME FRACTION:
Option = Value
Volume Fraction = 1
END
END
END
FLUID: SCCO2
BOUNDARY CONDITIONS:
VOLUME FRACTION:
Option = Value
Volume Fraction = 0
END
END
END
END
DOMAIN MODELS:
BUOYANCY MODEL:
Buoyancy Reference Density = 490 [kg m^-3]
Gravity X Component = 0 [m s^-2]
Gravity Y Component = -9.81 [m s^-2]
Gravity Z Component = 0 [m s^-2]
Option = Buoyant
BUOYANCY REFERENCE LOCATION:
Option = Automatic
END
END
DOMAIN MOTION:
Option = Stationary
END
MESH DEFORMATION:
Option = None
END
REFERENCE PRESSURE:
Reference Pressure = 1 [atm]

END
END
FLUID DEFINITION: Brine
Material = Brine
Option = Material Library
MORPHOLOGY:
Option = Continuous Fluid
END
END
FLUID DEFINITION: SCCO2
Material = SCCO2
Option = Material Library
MORPHOLOGY:
Option = Continuous Fluid
END
END
FLUID MODELS:
COMBUSTION MODEL:
Option = None
END
FLUID: Brine
FLUID BUOYANCY MODEL:
Option = Density Difference
END
END
FLUID: SCCO2
FLUID BUOYANCY MODEL:
Option = Density Difference
END
END
HEAT TRANSFER MODEL:
Homogeneous Model = False
Option = None
END
THERMAL RADIATION MODEL:
Option = None
END
TURBULENCE MODEL:
Homogeneous Model = False
Option = Laminar
END
END
FLUID PAIR: Brine | SCCO2
Surface Tension Coefficient = 0.0262 [N m^-1]
INTERPHASE TRANSFER MODEL:
Option = Free Surface
END
MASS TRANSFER:
Option = None
END
MOMENTUM TRANSFER:
DRAG FORCE:
Drag Coefficient = 0.44

Option = Drag Coefficient
END
END
SURFACE TENSION MODEL:
Option = Continuum Surface Force
Primary Fluid = Brine
END
END
MULTIPHASE MODELS:
Homogeneous Model = Off
FREE SURFACE MODEL:
Option = Standard
END
END
END

END